

**DEVELOPMENT OF ENHANCING  
HORIZONTAL RESOLUTION (EHR)  
TECHNIQUE IN 2-D RESISTIVITY SURVEY**

**NORDIANA MOHD MUZTAZA**

**UNIVERSITI SAINS MALAYSIA**

**2013**

**DEVELOPMENT OF ENHANCING HORIZONTAL RESOLUTION (EHR)  
TECHNIQUE IN 2-D RESISTIVITY SURVEY**

**by**

**NORDIANA MOHD MUZTAZA**

**Thesis submitted in fulfillment of the  
requirements for the degree of  
Doctor of Philosophy**

**JULY 2013**

## ACKNOWLEDGEMENTS

First and foremost Praise to Allah. I would like to express my sincere gratitude to my main supervisor, Dr. Rosli Saad for the continuous support of my Ph.D study and research, for his patience, motivation, enthusiasm and immense knowledge. His guidance helped me in all the time of research and writing of this thesis. One simply could not wish for a better or friendlier supervisor. Besides my main supervisor, I would like to thank my co-supervisor, Prof. Dr. Mohd. Nawawi Mohd Nordin for being supportive, insightful comments and give his great help all the time. Prof. Dr. Mokhtar Saidin from Centre for Archaeological Research (CGAR) greatly helped me with the archaeological aspect and providing so much information whenever possible.

My sincere thanks also go to Geophysics lab staff Mr. Mydin Jamal, Mr. Yaakob Othman, Mr. Low Weng Leng, Mr. Shahil Ahmad Khosaini and Mr. Azmi Abdullah for scarifying their time and energy assisting me in the projects.

In my daily work I have been blessed with a helpful, friendly and cheerful group of fellow friends in Geophysics course mate, Ms. Nur Azwin Ismail, Ms. Noer El Hidayah Ismail, Mr. Andy Anderson Bery, Ms. Teh Saufia Abu Hasim Ajau'ubi, Ms. Khairun Nisa' Ahmad Ali, Mr. Mark Jinmin, Mr. Kiu Yap Chong, Mr. Ragu Ragava Rao A/L Satinaranan and Mr. Shyeh Sahibul Karamah Masnan.

Further and the most important, million thanks to my family: my parents Mohd Muztaza Yahya and Sarimah Salim, my siblings Norlita Zaiyana, Mohd

Khairul, Norhidayahti, Ilani, Nas Rashidah and Maisarah for their prayers, support and understanding during my study.

Finally, I would like to thank the Academic Staff Training Scheme (ASTS), Universiti Sains Malaysia (USM) and Kementerian Pengajian Tinggi (KPT) for their sponsorship of my studies and the Postgraduate Research Grant Scheme (PRGS), USM have funded my research.

# CONTENTS

	<b>Page</b>
Acknowledgements	ii
Contents	iv
List of table	viii
List of figure	ix
List of photo	xviii
List of symbol	xx
List of abbreviation	xxi
Abstrak	xxii
Abstract	xxiv
CHAPTER 1 INTRODUCTION	1
1.0 Background	1
1.1 Problem statements	5
1.2 Research objectives	6
1.3 Significance and novelty of the study	6
1.4 Layout of thesis	7
CHAPTER 2 LITERATURE REVIEW	9
2.0 Introduction	9
2.1 Resistivity theory	10
2.1.1 Current flow from two closely spaced electrodes	12
2.1.2 Measuring earth resistivity	14
2.1.3 Depth of penetration.	15
2.1.4 Current flow in layered media	16
2.1.5 Current flow and current density	17
2.1.6 Current flow and electrode spacing	19

	2.1.7	Resistivity arrays	23
	2.1.8	The relationship between geology and resistivity	26
2.2		Previous work	28
2.3		Summary	37
CHAPTER 3 RESEARCH METHODOLOGY			39
3.0		Preface	39
3.1		Testing models	45
	3.1.1	Simulation model	45
	3.1.2	Miniature model	45
	3.1.3	Field model	46
	3.1.4	Test model	46
3.2		2-D Resistivity process	47
3.3		Field study	48
	3.3.1	Archaeology	49
	3.3.2	Mineral exploration	53
	3.3.3	Engineering and environment	55
	3.3.4	Geology	62
3.4		Data acquisition	66
	3.4.1	2-D resistivity	68
	3.4.2	2-D resistivity with EHR technique	70
3.5		Survey lines	72
	3.5.1	Archaeology	73
	3.5.2	Mineral exploration	77
	3.5.3	Engineering and environment	78
	3.5.4	Geology	83
3.6		Chapter summary	86

CHAPTER 4	RESULTS AND DISCUSSIONS	87
4.0	Basis	87
4.1	Testing models	87
	4.1.1 Simulation model	89
	4.1.1.1 Numerical comparison	94
	4.1.1.2 Discussion of simulation model	99
	4.1.2 Miniature model	100
	4.1.2.1 Discussion of miniature model	104
	4.1.3 Field model	106
	4.1.3.1 Discussion of field model	109
	4.1.4 Test model	112
	4.1.4.1 Discussion of test model	115
4.2	Field study	115
	4.2.1 Archaeology	116
	4.2.2 Mineral exploration	129
	4.2.3 Engineering and environment	133
	4.2.4 Geology	159
4.3	Summary	165
CHAPTER 5	CONCLUSION AND RECOMMENDATIONS	172
5.0	Conclusion	172
5.1	Recommendations	174
REFERENCES		175

APPENDIX A - Borehole records at Bukit Bunuh, Lenggong, Perak

APPENDIX B - Borehole records at Batang Merbau, Tanah Merah, Kelantan

APPENDIX C - Borehole records at Puchong, Selangor

APPENDIX D - Borehole records at Putra Heights, Damansara, Selangor

APPENDIX E - Borehole records at Southern Industrial & Logistics Clusters (SiLC),  
Nusajaya, Johor

LIST OF PUBLICATION

LIST OF AWARDS



## LIST OF TABLE

		<b>Page</b>
Table 2.1	Current path and their percent of total current that penetrates into the depth of line (modified after Burger, 1992; Robinson and Coruh, 1988; Telford et al., 1990)	13
Table 2.2	Resistivity of some common rocks and soil materials in survey area (Keller and Frischknecht, 1996)	26
Table 2.3	Electrical resistivity of some types of waters (Keller and Frischknecht, 1996)	27
Table 2.4	Chargeability and resistivity of some common rocks and minerals (Modified from Reynolds, 1997; Telford and Sheriff, 1984)	27
Table 3.1	Coordinate of the study location	51
Table 3.2	List of equipment of 2-D resistivity method	67
Table 4.1	Results of four types of common arrays and modified arrays with EHR technique	105
Table 4.2	Summary of results obtained using 2-D resistivity with/ without EHR technique from eight study areas	168

## LIST OF FIGURE

		<b>Page</b>
Figure 2.1	A conventional four electrode array to measure the subsurface resistivity (modified after Loke, 1997)	10
Figure 2.2	Measuring earth resistivity (modified after Burger, 1992; Robinson and Coruh, 1988; Telford et al., 1990)	12
Figure 2.3	Equipotential surfaces (black lines) and current lines of flow (red lines) (modified after Burger, 1992; Robinson and Coruh, 1988; Telford et al., 1990)	13
Figure 2.4	Four electrodes principle to measure resistivity or conductivity (modified after Burger, 1990; Pozdnyakova and Zhang, 1999; Butler, 2001)	14
Figure 2.5	Potential along the surface and potential difference (modified after Burger, 1990; Pozdnyakova and Zhang, 1999; Butler, 2001)	14
Figure 2.6	Current flow through the earth with different electrode spacing (After Burger, 1992)	15
Figure 2.7	Current flows through a model of high resistivity overlying low resistivity layer (modified after Burger, 1992)	16
Figure 2.8	Current flows through a model of low resistivity overlying high resistivity layer (modified after Burger, 1992)	17
Figure 2.9	Refraction of current flow lines at a boundary separating materials of different resistivity. (a) Symbols used in equation 4.6, (b) Refraction when $\rho_1 < \rho_2$ , (c) Refraction when $\rho_1 > \rho_2$  (modified after Burger, 1992)	18
Figure 2.10	Qualitative distribution of current flow lines when a horizontal interface separates materials of different resistivities. (a) Homogeneous subsurface, (b) $\rho_2 > \rho_1$ , (c) $\rho_2 < \rho_1$ (modified after Burger, 1992)	19
Figure 2.11	Current flow through different resistivity medium with different electrode spacing (modified from Burger, 1992)	20
Figure 2.12	Apparent resistivity with electrode spacing in high resistivity layer (Mooney, 1958 as cited by Reynolds, 1997)	21

Figure 2.13	Current flow through lower to higher resistivity medium with different electrode spacing (modified after Burger, 1992)	22
Figure 2.14	Apparent resistivity with electrode spacing in low resistivity layer (Mooney, 1958 as cited by Reynolds, 1997)	23
Figure 2.15	Common arrays used in resistivity surveys and their geometric factors	24
Figure 2.16	The three different models used in the interpretation of resistivity measurements (modified after Loke, 1994)	25
Figure 2.17	A typical 1-D model used in the interpretation of resistivity sounding data for Wenner array (modified after Loke, 1994)	25
Figure 2.18	Resistivity and conductivity values of some common rocks (Palacky, 1987)	26
Figure 3.1	Research methodology flowchart for development of EHR technique	40
Figure 3.2	Current flow through the earth after using the 2-D resistivity technique with EHR technique	41
Figure 3.3	The arrangement of electrodes for a resistivity survey and the sequence of measurements, a) first stage of data acquisition with 'a' spacing, b) second stage of data acquisition (move 'a/2' with 'a' spacing) and c) combination of data to build up a detail pseudo section (EHR)	42
Figure 3.4	The arrangement of electrodes for a resistivity survey and the sequence of measurements for Wenner array, a) datum points for common array, b) datum points for EHR technique to build up a detailed pseudo section	43
Figure 3.5	The arrangement of electrodes for a resistivity survey and the sequence of measurements for Schlumberger array, a) datum points for common array, b) datum points for EHR technique to build up a detailed pseudo section	43
Figure 3.6	The arrangement of electrodes for a resistivity survey and the sequence of measurements for Wenner-Schlumberger array, a) datum points for common array, b) datum points for EHR technique to build up a detailed pseudo section	44
Figure 3.7	The arrangement of electrodes for a resistivity survey and the sequence of measurements for Pole-dipole array, a) datum points for common array, b) datum points for EHR technique to build up a detailed pseudo section	44

Figure 3.8	Example of the produced resistivity section a) Measured, b) Calculated and c) Inversion by RES2DINV	48
Figure 3.9	Location of eight study areas (Google earth, 2012)	49
Figure 3.10	Geology map of Sungai Batu, Kedah (Geological Map of Peninsular Malaysia. Minerals and Geoscience Department Malaysia. 8 <sup>th</sup> Edition, 1985)	50
Figure 3.11	Location of study area at Lembah Bujang, Kedah (Google Earth, 2012)	51
Figure 3.12	Geology map of Bukit Bunuh, Lenggong, Perak	52
Figure 3.13	Study area located at Bukit Bunuh, Perak (Google Earth, 2012)	53
Figure 3.14	Geology map of Pagoh, Johor (Geological Map of Peninsular Malaysia. Minerals and Geoscience Department Malaysia. 8 <sup>th</sup> Edition, 1985).	54
Figure 3.15	Study area located in Pagoh, Batu Pahat, Johor (Google Earth, 2012).	55
Figure 3.16	Geology map of Batang Merbau, Tanah Merah, Kelantan (Geological Map of Peninsular Malaysia. Minerals and Geoscience Department Malaysia. 8 <sup>th</sup> Edition, 1985)	57
Figure 3.17	Study area at Batang Merbau, Tanah Merah, Kelantan (Google Earth, 2012)	58
Figure 3.18	Geology of Selangor	59
Figure 3.19	Study area at Puchong, Selangor (Google Earth, 2012)	60
Figure 3.20	Geology of the Putra Heights area	61
Figure 3.21	Study area located at Putra Heights, Selangor	62
Figure 3.22	Geology of the Nusajaya area	63
Figure 3.23	Study area located at SiLC, Nusajaya, Johor	64
Figure 3.24	Geology map of Beseri, Kaki Bukit, Perlis	65
Figure 3.25	Study area located at Beseri, Kaki Bukit, Perlis	66
Figure 3.26	Two ABEM cables with sequence measurement to build up pseudo section (After ABEM, 2009)	69

Figure 3.27	Four ABEM cables with sequence measurement to build up pseudo section (After ABEM, 2009)	69
Figure 3.28	Cable arrangement for roll-along method with sequence measurement to build up pseudo section (After ABEM, 2009)	69
Figure 3.29	Two ABEM cables with sequence measurement PDP4S to build up pseudo section with EHR technique	70
Figure 3.30	Four ABEM cables with sequence measurement PDP4L to build up pseudo section with EHR technique	71
Figure 3.31	Four ABEM cables with sequence measurement PDP4S and PDP4L to build up pseudo section with EHR technique	71
Figure 3.32	Survey lines of 2-D resistivity at Sungai Batu, Lembah Bujang	73
Figure 3.33	2-D resistivity survey lines at Bukit Bunuh, Lenggong, Perak	75
Figure 3.34	Electrical method survey lines at Pagoh, Batu Pahat, Johor (Google Earth, 2012)	77
Figure 3.35	The four parallel 2-D resistivity survey lines and borehole at Batang Merbau, Tanah Merah, Kelantan	79
Figure 3.36	Map of study area showing 2-D resistivity profile lines (PR1 and PR2) and borehole location (DBH 1 to DBH 7) (Google Earth, 2012)	80
Figure 3.37	Survey lines with borehole at Putra Heights, Selangor	82
Figure 3.38	2-D resistivity with EHR technique and borehole location at SiLC, Nusajaya, Johor	84
Figure 3.39	2-D resistivity survey lines at Beseri, Kaki Bukit, Perlis	85
Figure 4.1	A block (anomalous) was created at 2-2.3 m and 0.1 m electrode spacing using Wenner array; a) model, b) apparent resistivity pseudo section and c) Inversion model resistivity (depth, m versus distance, m)	89
Figure 4.2	A block (anomalous) was created at 2-2.3 m and 0.1 m electrode spacing using Wenner-Schlumberger array; a) model, b) apparent resistivity pseudo section and c) Inversion model resistivity (depth, m versus distance, m)	90
Figure 4.3	A block (anomalous) was created at 2-2.3 m and 0.1 m electrode spacing using Pole-dipole array; a) model, b) apparent resistivity pseudo section (forward), c) apparent resistivity pseudo section (reverse) model and d) Inversion model resistivity (depth, m versus distance, m)	91

Figure 4.4	A block (anomalous) was created at 2.05-2.3 m and 0.1 m electrode spacing using Wenner array; a) model, b) apparent resistivity pseudo section and c) Inversion model resistivity (depth, m versus distance, m)	92
Figure 4.5	A block (anomalous) at 2.05-2.3 m and 0.1 m electrode spacing using Wenner-Schlumberger array; a) model, b) apparent resistivity pseudo section and c) Inversion model resistivity (depth, m versus distance, m)	92
Figure 4.6	A block (anomalous) was created at 2.05-2.3 m and 0.1 m electrode spacing using Pole-dipole array; a) model, b) apparent resistivity pseudo section (forward), c) apparent resistivity pseudo section (reverse) model and d) Inversion model resistivity (depth, m versus distance, m)	93
Figure 4.7	Inversion model resistivity (depth, m versus distance, m) with 0.05 m electrode spacing using Wenner array with EHR technique	94
Figure 4.8	Inversion model resistivity (depth, m versus distance, m) with 0.05 m electrode spacing using Wenner- Schlumberger array with EHR technique	94
Figure 4.9	Inversion model resistivity (depth, m versus distance, m) with 0.05 m electrode spacing using Pole-dipole array with EHR technique	94
Figure 4.10	A resolution of theoretical model with and without EHR technique using Wenner array; a) Resistivity versus depth b) Resistivity versus x-distance	96
Figure 4.11	A resolution of theoretical model with and without EHR technique using Wenner-Schlumberger array; a) Resistivity versus depth b) Resistivity versus x-distance.	97
Figure 4.12	A resolution of theoretical model with and without HER technique using Pole-dipole array; a) Resistivity versus depth b) Resistivity versus x-distance	98
Figure 4.13	The sketch of hole dimension	101
Figure 4.14	Inversion model resistivity before the hole was created using a) Wenner b) Schlumberger c) Wenner-Schlumberger d) Pole-dipole array	102
Figure 4.15	Inversion model resistivity with a hole in miniature model using a) Wenner b) Schlumberger c) Wenner-Schlumberger	

	d) Pole-dipole array	103
Figure 4.16	Inversion model resistivity with a hole in miniature model using EHR technique a) Wenner b) Schlumberger c) Wenner-Schlumberger d) Pole-dipole array	104
Figure 4.17	The sketch of survey line at Bunker, Desasiswa Bakti Permai, USM for Pole-dipole short, Pole-dipole long and Pole-dipole long-short arrays at the same survey line with front view	107
Figure 4.18	Inversion model resistivity of bunker using Pole-dipole short array without EHR technique	108
Figure 4.19	Inversion model resistivity of bunker using Pole-dipole short array with EHR technique	108
Figure 4.20	Inversion model resistivity of bunker using Pole-dipole long array without EHR technique	108
Figure 4.21	Inversion model resistivity of bunker using Pole-dipole long array with EHR technique.	109
Figure 4.22	Inversion model resistivity of bunker using Pole-dipole long-short array	109
Figure 4.23	The inversion model resistivity for a) short b) long and c) long-short array (After Bernard, 2003) without EHR technique	111
Figure 4.24	The inversion model resistivity for a) short and b) long array with EHR technique	111
Figure 4.25	Inversion model resistivity of underground drainages where the x-axis represents distance (m) and y-axis represents depth (m); a) Wenner array b) Wenner array with EHR technique	113
Figure 4.26	Inversion model resistivity of underground drainages where the x-axis represents distance (m) and y-axis represents depth (m); a) Schlumberger array b) Schlumberger array with EHR technique	113
Figure 4.27	Inversion model resistivity of underground drainages where the x-axis represents distance (m) and y-axis represents depth (m); a) Wenner-Schlumberger array b) Wenner-Schlumberger with EHR technique	114
Figure 4.28	Inversion model resistivity of underground drainages where the x-axis represents distance (m) and y-axis represents depth (m); a) Pole-dipole array b) Pole-dipole array with EHR technique	114

Figure 4.29	Inversion model of resistivity (depth, m versus distance, m) of LBR8 a) without EHR b) with EHR technique using Pole-dipole long array	116
Figure 4.30	Inversion model resistivity (depth, m versus distance, m) of LBR1-LBR7 from 2-D resistivity survey line with EHR technique using Pole-dipole long array	117
Figure 4.31	Inversion model resistivity (depth, m versus distance, m) of LBR8-LBR10 from 2-D resistivity survey line with EHR technique using Pole-dipole long array	118
Figure 4.32	The ancient river with two type of sediment	119
Figure 4.33	Inversion model of 2-D resistivity (depth, m versus distance, m) a) without EHR b) with EHR technique	121
Figure 4.34	Inversion model of 2-D resistivity (depth, m versus distance, m) a) without HER b) with EHR technique	122
Figure 4.35	Resistivity section (depth, m versus distance, m) of West-East direction (BBR1), 8 km (0-1200 m, Grik Highway, 1385-1995 m, Road to Lenggong, 2095-3730 m, Sungai Perak, 4010-5850 m, Batu Sapi Highway, 6010-8020 m)	124
Figure 4.36	Resistivity section (depth, m versus distance, m) of North-West to South-East line (BBR2), 0-1135 m	125
Figure 4.37	Resistivity section (depth, m versus distance, m) of North-West to South-East line (BBR2), 1135-6610 m	126
Figure 4.38	Resistivity section (depth, m versus distance, m) of South-West to North-East line (BBR3), 0-1840 m	127
Figure 4.39	Resistivity topography map; a) ground surface, b) bedrock	127
Figure 4.40	3-D image of overburden of study area	128
Figure 4.41	3-D image of topography and survey lines	128
Figure 4.42	3-D image of rock head topography and survey lines of study area	129
Figure 4.43	a) Inversion model resistivity (depth, m versus distance, m) of PAR1 without EHR technique from electrical resistivity and b) chargeability section from IP survey	131
Figure 4.44	a) Inversion model resistivity (depth, m versus distance, m) of PAR1 with EHR technique from electrical resistivity and b) chargeability section from IP survey	131



Figure 4.45	2-D inversion model resistivity (depth, m versus distance, m) of BMR1-BMR4 without EHR technique at Batang Merbau, Tanah Merah, Kelantan	134
Figure 4.46	2-D inversion model resistivity (depth, m versus distance, m) of survey lines BMR1-BMR4 with EHR technique at Batang Merbau, Tanah Merah, Kelantan	135
Figure 4.47	2-D inversion model resistivity (depth, m versus distance, m) of survey line of BM1-BM4 at Batang Merbau, Tanah Merah, Kelantan	136
Figure 4.48	Borehole record for DBH4	137
Figure 4.49	Inversion model resistivity (depth, m versus distance, m) of PR1 with correlation of DBH4; a) without EHR technique and b) with EHR technique	139
Figure 4.50	Inversion model resistivity (depth, m versus distance, m) of PR1 with SPT N-value; a) Pole-dipole array b) Pole-dipole array with EHR technique	140
Figure 4.51	Relationship between measured N-values and resistivity of PR1 a) without EHR technique b) with EHR technique	141
Figure 4.52	Inversion model resistivity (depth, m versus distance, m) of PR2; a) without EHR technique and b) with EHR technique	142
Figure 4.53	BH3 located at 30 m of PHR1, Putra Heights, Selangor	144
Figure 4.54	Resistivity section (depth, m versus distance, m) of PHR1 with correlation of BH3 and BH5; a) without EHR technique and b) with EHR technique at Putra Heights, Selangor	147
Figure 4.55	Resistivity section (depth, m versus distance, m) of PHR2 with correlation of BH3; a) without EHR technique and b) with EHR technique at Putra Heights, Selangor	150
Figure 4.56	Correlation of resistivity section (depth, m versus distance, m) of PHR7, BH3 and BH5 at Putra Heights, Selangor; a) without EHR technique and b) with EHR technique	153
Figure 4.57	Relationship between SPT N-value for BH3 and resistivity section of PHR1; a) without b) with EHR technique at Putra Heights, Selangor	154
Figure 4.58	Relationship between SPT N-value for BH5 and resistivity section of PHR1; a) without b) with EHR technique at Putra Heights, Selangor	155

Figure 4.59	Correlation of resistivity section (depth, m versus distance, m) of PHR2 and BH3 at Putra Heights, Selangor; a) without EHR technique and b) with EHR technique	157
Figure 4.60	Relationship between SPT N-value for BH3 and resistivity section of PHR2; a) without b) with EHR technique at Putra Heights, Selangor	158
Figure 4.61	Resistivity section (depth, m versus distance, m) of PHR3 at Putra Heights, Selangor; a) without EHR and b) with EHR technique	159
Figure 4.62	2-D inversion model resistivity (depth, m versus distance, m) of SR8; a) without EHR technique b) with EHR technique at SiLC, Nusajaya, Johor	160
Figure 4.63	Inversion model resistivity (depth, m versus distance, m) of the outcrop with EHR technique at SiLC, Nusajaya, Johor	162
Figure 4.64	Contouring model resistivity (depth, m versus distance, m) for sedimentary deposits at SiLC, Nusajaya, Johor	162
Figure 4.65	2-D inversion model resistivity (depth, m versus distance, m) of PER1; a) without EHR technique b) with EHR technique	163
Figure 4.66	2-D inversion model resistivity (depth, m versus distance, m) of PER2; a) without EHR technique b) with EHR technique	164
Figure 4.67	Inversion model resistivity (depth, m versus distance, m) at Beseri, Kaki Bukit, Perlis	165
Figure 4.68	Contouring model resistivity (depth, m versus distance, m) for limestone deposits at Beseri, Kaki Bukit, Perlis	165

## LIST OF PHOTO

		<b>Page</b>
Photo 3.1	Equipments of 2-D resistivity method	67
Photo 3.2	2-D resistivity survey line at Lembah Bujang, Kedah	74
Photo 3.3	2-D resistivity survey line at Bukit Bunuh, Lenggong, Perak	76
Photo 3.4	2-D resistivity and IP survey line at Pagoh, Batu Pahat, Johor	78
Photo 3.5	2-D resistivity survey line at Batang Merbau, Kelantan	80
Photo 3.6	2-D resistivity at Putra Height, Selangor	83
Photo 3.7	2-D resistivity survey line at SiLC, Nusajaya, Johor	84
Photo 3.8	2-D resistivity survey line at Kaki Bukit, Beseri, Perlis	85
Photo 4.1	Miniature model without a hole	101
Photo 4.2	Miniature model with a hole	101
Photo 4.3	Resistivity survey carried out at miniature model	102
Photo 4.4	Bunker at Desasiswa Bakti Permai, USM as a second model	107
Photo 4.5	Test site with underground drainages	112
Photo 4.6	Residual soil at the study area	131
Photo 4.7	A sample of iron ore found at the study area	132
Photo 4.8	Iron ore excavation process	133
Photo 4.9	The weathered rocks with secondary iron ore deposit found after excavation	133
Photo 4.10	Sample of affected building structure from the area	143
Photo 4.11	Tension crack on the road near to the retaining wall	143
Photo 4.12	Sedimentation outcrop at SiLC, Nusajaya, Johor	162



## LIST OF SYMBOL

I	Current
V	Potential
$\rho_a$	Apparent resistivity
$\varepsilon$	Electric conductivity
k	Geometric factor
R	Configuration resistance
r	Distance between the current electrodes
$\Omega\text{m}$	Ohm-meter
cm	centimeter
Hz	Hertz
m	Meter
km	kilometer
$\mu$	Poisson's ratio
G	Rigidity modulus
E	Elastic coefficients
$\rho$	Density
v	Velocity
K	Bulk modulus
$v_n$	Velocity of n-layer
h	Thickness
$h_n$	Thickness of n-layer
$\theta_i$	Refraction angle
$\theta_{ic}$	Incidence critical angle
$\theta_{cn}$	Critical angle of layer n <sup>th</sup>
t	Time
$t_i$	Intercept time
$t_{id}$	Intercept time of down-dip
$t_{iu}$	Intercept time of up-dip
$\beta$	Dipping angle
$x_c$	Critical distance
>	More than
<	Less than

## LIST OF ABBREVIATION

1-D	One dimensional
2-D	Two dimensional
3-D	Three dimensional
VES	Vertical Electrical Sounding
C	Current electrode
P	Potential electrode
EHR	Enhancing Horizontal Resolution
RES2DMOD	Resistivity 2-D Modeling software
RES2DINV	Resistivity 2-D Inversion software
SAS4000	Signal Averaging System 4000
USM	Universiti Sains Malaysia
IP	Induced polarization
SP	Self-Potential
m/s	unit meter per second
MSL	Mean sea level
MY	Million years ago
DC	Direct current
ACS	Atlantic continental shelf
SPT	Standard penetration test
SiLC	Southern Industrial & logistics Clusters
CGAR	Centre for Global Archaeological Research (CGAR)
JMG	Jabatan Mineral dan Geosains Malaysia
LBR	Lembah Bujang with 2-D resistivity survey
BBR	Bukit Bunuh with 2-D resistivity survey
PAR	Pagoh with resistivity 2-D survey
BMR	Batang Merbau with 2-D resistivity survey
PR	Puchong with resistivity 2-D survey
PHR	Putra Heights with resistivity 2-D survey
SR	Southern Industrial & logistics Clusters (SiLC), Nusajaya with 2-D resistivity survey
PER	Beseri, Kaki Bukit, Perlis with 2-D resistivity survey

# **MEMBANGUNKAN TEKNIK PENINGKATAN RESOLUSI MENDATAR (EHR) DALAM SURVEI KEBERINTANGAN 2-D**

## **ABSTRAK**

Kajian keberintangan 2-D adalah satu kaedah tidak langsung dalam kajian subpermukaan cetek untuk mengekalkan geo-persekitaran. Ianya digunakan untuk mengukur keberintangan ketara subpermukaan. Kajian ini melibatkan pengubahsuaian teknik pengambilan data keberintangan 2-D dengan menggunakan empat susunatur yang berbeza (Wenner, Schlumberger, Wenner-Schlumberger dan Pole-dipole). Teknik ini dinamakan Peningkatan Resolusi Mendatar (EHR). Teknik EHR direka bagi mendapatkan penembusan yang lebih jelas dan dalam untuk kajian subpermukaan cetek. Empat model telah direka dan disahkan untuk mengkaji keberkesanan teknik EHR yang terdiri daripada satu model komputer dengan menggunakan perisian RES2DMOD dan tiga model lapangan; model lapangan (bersaiz kecil) dalam medium asal, bunker dan sistem pengairan bawah tanah. Penyongsangan model keberintangan dengan susunatur biasa menunjukkan resolusi mendatar yang kurang berbanding penyongsangan model keberintangan dengan menggunakan teknik EHR. Hasil daripada teknik EHR menunjukkan imej dan lapisan anomali yang jelas dari segi saiz, kedalaman dan nilai keberintangan. Oleh itu, penyongsangan ke atas model data yang lebih tepat menggunakan teknik ini boleh dilaksanakan dan tapak kajian dalam bidang arkeologi, eksplorasi mineral, kejuruteraan, persekitaran dan geologi menggunakan teknik EHR telah dijalankan. Lapan lokasi yang berbeza telah dikenal pasti yang kebanyakannya tertumpu pada kajian subpermukaan cetek. Lokasi tersebut adalah Lembah Bujang, Kedah; Bukit Bunuh, Lenggong, Perak; Pagoh, Batu Pahat, Johor; Batang Merbau, Tanah Merah,

Kelantan; Puchong, Selangor; Putra Heights, Selangor; Nusajaya, Johor dan Kaki Bukit, Perlis. Oleh itu, kajian keberintangan 2-D menggunakan susunatur Pole-dipole dengan teknik EHR dan tanpa teknik EHR telah dijalankan kerana mempunyai resolusi mendatar dan menegak yang baik dengan korelasi rekod lubang bor. Teknik EHR menghasilkan penembusan kedalaman yang hampir sama dengan teknik tanpa EHR walaupun teknik EHR menggunakan jarak elektrod minimum yang lebih kecil. Tambahan pula, ia meningkatkan resolusi mendatar. Terdapat korelasi yang baik antara kajian keberintangan 2-D dengan teknik EHR dan keputusan rekod lubang bor. Teknik EHR telah berjaya diaplikasi untuk sasaran yang besar dan kecil yang terletak pada kedalaman yang cetek atau dalam yang berkaitan dengan kajian arkeologi, eksplorasi mineral, kejuruteraan, persekitaran dan geologi yang sebelumnya mustahil dipetakan.



# **DEVELOPMENT OF ENHANCING HORIZONTAL RESOLUTION (EHR) TECHNIQUE IN 2-D RESISTIVITY SURVEY**

## **ABSTRACT**

2-D resistivity method is an indirect method to the shallow subsurface survey for maintaining the geo-environment. It is used to measure the apparent resistivity of subsurface. The research involves modified 2-D resistivity acquisition technique using four different arrays (Wenner, Schlumberger, Wenner-Schlumberger and Pole-dipole). This technique is called Enhancing Horizontal Resolution (EHR). The EHR technique was developed in order to acquire detail and deeper penetration for shallow subsurface study. Four models were designed and validate to study the effectiveness of EHR technique which consists of one computer model using RES2DMOD software and three field models; miniature with original medium, bunker and underground drainages. Inversion model resistivity with common array shows less horizontal resolution compared to inversion model resistivity with EHR technique. Results from the EHR technique shows clear images of an anomalous and layers in terms of size, depth and resistivity value. Notably, the technique can perform the inversion on model data set efficiency and for archaeology, mineral exploration, engineering, environment and geology, the EHR technique employed. Eight different locations were identified which were mainly focused on shallow subsurface investigations. The locations are Lembah Bujang, Kedah; Bukit Bunuh, Lenggong, Perak; Pagoh, Batu Pahat, Johor; Batang Merbau, Tanah Merah, Kelantan; Puchong, Selangor; Putra Heights, Selangor; Nusajaya, Johor and Kaki Bukit, Perlis. Throughout, 2-D resistivity with Pole-dipole array with and without EHR technique was adopted for this study due to the good horizontal and vertical

resolution with correlation of borehole records. EHR technique produces the same depth of penetration as without EHR technique although it used smaller minimum electrode spacing. Furthermore it enhances the horizontal resolution. There is a good correlation between the 2-D resistivity investigations with EHR technique and the results of borehole records. The EHR technique was successfully apply for larger and smaller target located at shallow or deeper depth which is associated with archaeology, mineral exploration, engineering, environment and geology studies that were previously impossible to map.

# CHAPTER 1

## INTRODUCTION

### 1.0 Background

Malaysia is a developing country, which requires extensive infrastructures and industrial development. Most favorable lands with strategic locations have been developed, leaving only the more challenging grounds for present and future developments. These challenging grounds are either hilly terrain or land with underlying materials of notorious mechanical characteristics, such as soft compressible deposits, loose granular deposits, brown fills, karstic limestone, waste dumps and peaty soil. In addition to these inherent unfavorable ground properties, project clients and local authorities have also demanded a more technically challenging criteria for the designs to ensure safety. The forms of structure proposed in this modern day demand taller and heavier structures, deeper foundation and underground excavation (Liew, 2010). Therefore, for projects involving subsurface or substructure works with foundation and underground space excavation; site formation with cut slope, fill, retaining structures and ground improvement works, geotechnical engineer and geophysicist are usually engaged. Geotechnical studies are usually used for subsurface, engineering and environmental works. Geophysical studies provide supported data for engineers to improve the work, cost saving and time. Geophysical studies can be used to determine depth of bedrock, the nature of overburden materials and near surface structures such as sinkholes, cavities, voids,

faults and boulders. Selection of the appropriate geophysical method has to be based on project objectives and site conditions to produce a good result.

Geophysical method is one of the fastest, most effective and least costly. The shallow subsurface of the earth is an extremely important zone that supports our infrastructure and provides for our industries. Infrastructure applications have more of an “Engineering” component, that is, dealing with the detection and characterization of dangerous roadbed conditions underlying highways. This type of application may involve detecting void under roadways due to underground (mining or tunneling) excavations, or characterizing the relative integrity of reinforced structures in bridges or other transportation structures. As safe and effective use of the near-surface environment is a major challenge facing our society, there is a great need to improve our understanding of the shallow subsurface. Many advances associated with near-surface geophysics have been made in the last decade (Bullock, 1988). These advanced methods (2-D resistivity, IP, SP, seismic, GPR, magnetic and gravity) which facilitate the use of geophysical data include better understanding of geophysical responses for near-surface environments and improved digital technology acquisition. The improvements of geophysical methods for near-surface imaging, such as computational speed and capabilities are associated with processing, inversion, modeling and visualization of geophysical data.

Exploration geophysics is also used to map subsurface structure, elucidate the underlying structures, obtain spatial distribution of rock units, and detect structures such as faults, folds and intrusive rocks. This is an indirect method to perform the shallow subsurface study for maintaining the infrastructure and geo-environment.

Ground Penetrating Radar (GPR) is the most powerful archaeogeophysical technique. GPR allows the registration of such fine archaeological objects that are hard to see by eye and can be missed during archaeological excavation (Conyers, 2004). GPR also allows precise localization of small metal objects and determination of the metal by its conductivity. It has the highest resolution of all geophysical techniques. However, the interpretation of the signal is extremely complicated and requires years of experience and it cannot be used in conductive environment (like sea water). Limited penetration depth which depends on the soil humidity, usually it varies from 1 m in wet soil to 17 m in buildings (Conyers, 2004).

Seismic method is commonly used to detect rock velocities and quality, overburden thickness, rock rippability and bedrock depth. Seismic investigates the subsurface by generating arrival time and offset distance information to determine the path and velocity of the elastic disturbance in the ground. It is also depends on elastic properties (compactness, rigidity and pore content). Pores, gas and fractures reduce the velocity while pressure, water and oil increase the velocity value. Seismic method has a resolution limit which is associated with wavelength, distance and shielding by surface rocks. Seismic wave can resolve structures whose size is about  $\frac{1}{4}$  of their wavelength that affect the resolution. The resolution decreases with distance and high electrical conductivity will give strong velocity contrast (Hermann, 2004).

Magnetic method is an efficient and effective method to survey large areas for underground iron and steel objects such as tanks and barrels. Magnetic measurement of the earth's total magnetic field and local magnetic gradients are usually made with proton precession magnetometers at points along a line which should be oriented at a high angle to the suspected trend of structures. Gradient

measurements are less sensitive to deeper objects than total field measurements and magnetic measurements are susceptible to interference from steel pipes, fences, vehicles and buildings. The magnetic method does not give exact depth determination (Grauch and Lindrith, 2005).

A microgravity survey provides a measure of change in subsurface density. Natural variations in subsurface density include lateral changes in soil or rock density, buried channels, large fractures, faults and cavities. Data can be interpreted to provide estimates of depth, size and the nature of the anomaly. Irregular topography will produce artifacts in the data unless accounted for in the processing. Local sources of vibrations, wind, storms and distance earthquakes can produce interference (Butler, 1984).

2-D resistivity survey can be useful in detecting bodies of anomalous material or in estimating the depth of bedrock surfaces. In coarse, granular soil, the groundwater surface is generally marked by an abrupt change in water saturation and thus by a change of resistivity. In fine grained soils, however, there may be no such resistivity change coinciding with a piezometric surface. Generally, since the resistivity of a soil or rock is controlled primarily by the pore water conditions, there are wide ranges in resistivity for any particular soil or rock type, and resistivity values cannot be directly interpreted in terms of soil type or lithology. The 2-D resistivity method has some inherent limitations that affect the resolution and accuracy that may be expected from it (Beresnev et al., 2002).

Like all methods using measurements of a potential field, the value of a measurement obtained at any location represents a weighted average of the effects produced over a large volume of material, with the nearby portions contributing most

heavily. For these reasons, it is always advisable to use several complementary geophysical methods in an integrated exploration study rather than relying on a single exploration method.

## **1.1 Problem statements**

The present 2-D resistivity acquisition technique has a few disadvantages such as penetration depth which is related to electrode spacing, resolution and high level of noise. The smaller the electrode spacing, the higher the horizontal resolution but penetration is shallow. The larger the electrode spacing, the lower the horizontal resolution but it allows for deeper penetration.

The most commonly used arrays in the 2-D resistivity surveys are conventional arrays such as Wenner, Schlumberger or Dipole-dipole arrays. These arrays are often well understood in terms of their depths of investigations, lateral and vertical resolution and signal-to-noise ratios. Generally, the Wenner and Schlumberger arrays provide good vertical resolution for horizontal structures and high signal-to-noise data. Reversely, the Dipole-dipole and Pole-dipole arrays produce poorer vertical resolution and lower signal-to noise ratios, but have better lateral resolution (Barker, 1979; Dahlin and Zhou, 2004). However, these conventional arrays may not be the most appropriate and effective options when the time and number of measurements given for the survey is limited, or when an object at a specific location in the very complex structure becomes the target of the survey.

## **1.2 Research objectives**

The objectives of this study are;

- i. to develop a new data acquisition technique for better resolution and deeper penetration.
- ii. to validate a useful technique that can give better results for archaeology, mineral exploration, engineering, environment and geological purposes.
- iii. to compare the results of common array and array with Enhancing Horizontal Resolution (EHR) technique.

## **1.3 Significance and novelty of the study**

The research work namely Enhancing Horizontal Resolution (EHR) technique aims to modify the 2-D resistivity acquisition technique based on the arrays (Wenner, Schlumberger, Wenner-Schlumberger and Pole-dipole) provided. The technique provides a better result and enhances horizontal resolution image with deeper penetration and low noise level. With the newly introduced EHR technique, all arrays (Wenner, Schlumberger, Wenner-Schlumberger and Pole-dipole) can now be carried out to map complex geological structures (smaller target located at deeper depth) that were previously impossible to map.

However the limitation of EHR technique was the time constrain depending on the minimum electrode spacing use and it was mainly focus on horizontal resolution not vertically.



## 1.4 Layout of thesis

Generally, the contents of this dissertation are organized as follows;

Chapter 2 include theory of 2-D resistivity method and early studies using 2-D resistivity method applied to archeological, mineral exploration, engineering and environment problems are discussed.

Chapter 3 is devoted to research methodology of 2-D resistivity method. The research involves 2-D resistivity for common array and modified 2-D resistivity acquisition technique using four different arrays (Wenner, Schlumberger, Wenner-Schlumberger and Pole-dipole). This technique is called Enhancing Horizontal Resolution (EHR). The application of EHR technique at study areas (Lembah Bujang, Kedah; Bukit Bunuh, Lenggong, Perak; Pagoh, Batu Pahat, Johor; Batang Merbau, Tanah Merah, Kelantan; Puchong, Selangor; Nusajaya, Johor and Beseri, Kaki Bukit, Johor) using Pole-dipole array is also discussed. Borehole record was used as a correlation with 2-D resistivity as assessed by EHR technique. The survey was divided into subsurface study in archaeology, mineral exploration, engineering, environment and geology.

In Chapter 4, four models were tested with EHR technique using Wenner, Schlumberger, Wenner-Schlumberger and Pole-dipole arrays. It consists of one computer model and three field models. The first model is a simulation model created by RES2DMOD software using Wenner, Wenner-Schlumberger and Pole-dipole array. The first field miniature model with void was carried out with Wenner, Schlumberger, Wenner-Schlumberger and Pole-dipole arrays to see the suitability of the arrays selected. The second field model was conducted at USM bunker using

Pole-dipole (long and short) array to study the contrast of horizontal resolution and the effectiveness of subsurface structure mapping with EHR technique. The test model was evaluated at USM Convocation site to study underground drainages using four different arrays; Wenner, Schlumberger, Wenner-Schlumberger and Pole-dipole with common and EHR techniques. This chapter continues discussed the results of the 2-D resistivity with and without EHR technique for application in archaeology, mineral exploration, engineering, environment and geology.

Finally, Chapter 5 concluded the 2-D resistivity study with EHR technique including recommendations for future research.

## CHAPTER 2

### LITERATURE REVIEW

#### 2.0 Introduction

Resistivity prospecting involves the detection of surface effects produced by electric current flow in the ground. Using resistivity methods, one may measure potentials, currents and electromagnetic fields that occur naturally or are introduced artificially in the earth. Basically, it is the enormous variation electrical conductivity found in different rocks and minerals that make these techniques possible.

Geotechnical studies are usually used for subsurface, engineering and environmental works. Geophysical studies provide supported data in order to save cost and time. Geophysical methods can be used to determine depth of bedrock, nature of overburden materials and near surface structures such as sinkholes, cavities, voids, faults and boulders. Selection of the appropriate geophysical method is based on project objectives and site conditions. Electrical methods (IP, SP, 2-D/3-D resistivity) are used to detect groundwater, mapping subsurface and to determine the boulders or bedrock. An induced polarization (IP) survey is used to delineate municipal waste landfills while Self-Potential (SP) and resistivity are used to map seepage paths. Shallow seismic reflection technique has recently been used in bedrock mapping, detecting abandoned coal mine, detecting saturated zone during a pump test in an alluvial aquifer and mapping shallow faults. Seismic refraction is used to study shallow subsurface investigation such as bedrock and faults. Both techniques depend on the presence of contrast in the subsurface. In many cases, the

contrast occurs at boundaries between geologic layers including man-made boundaries such as tunnels and mines.

## 2.1 Resistivity theory

The purpose of the resistivity survey is to determine the subsurface resistivity distribution by making measurements on the ground surface. From these measurements, the true resistivity of the subsurface can be estimated. The ground resistivity is related to various geological parameters such as mineral and fluid content, porosity and degree of water saturation in rock. Resistivity surveys have been used for many decades in hydrological, mining and geotechnical investigations. More recently, it has been used for environmental surveys.

The resistivity measurements, shown in Figure 2.1 are normally made by injecting current into the ground through two current electrodes,  $C_1$  and  $C_2$  while measuring the resulting voltage difference at two potential electrodes  $P_1$  and  $P_2$ . From the current ( $I$ ) and potential ( $V$ ) values, an apparent resistivity ( $\rho_a$ ) value is calculated (2.1-2.3).

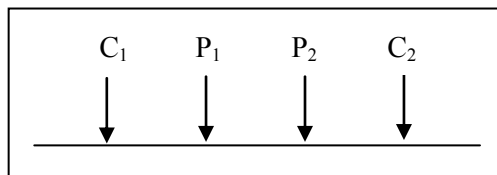


Figure 2.1: A conventional four electrode array to measure the subsurface resistivity (modified after Loke, 1997).

$$\rho_a = k V/I \quad (2.1)$$

Where  $k$  : Geometric factor (depends on the arrangement of four electrode)

$V$  : Potential

$I$  : Current

$\rho_a$ : Apparent resistivity

Resistivity meters normally give a resistance value,

$$R = V/I \quad (2.2)$$

So, in practice the apparent resistivity value is calculated by,

$$\rho_a = kR \quad (2.3)$$

The calculated resistivity value is not the true resistivity of the subsurface, but an apparent value which is the resistivity of a homogeneous ground with the same resistance value for the same electrode arrangement. The relationship between the apparent resistivity and the true resistivity is a complex relationship (Loke, 1997, 1999, 2000).

The potential change from a single current electrode to some point in the half space representing the earth can be calculated using Ohm's law (2.4) (Loke, 1997, 1999, 2000).

$$\begin{aligned} V &= IR \quad (2.4) \\ &= \frac{\rho I}{k} \\ &= \frac{\rho I}{2\pi r} \end{aligned}$$

Where  $V$  : Potential

$R$  : Resistance

$I$  : Current

$\rho$  : Resistivity

$k$  : Geometric factor

$r$  : Distance between the current electrodes

Earth resistivity can be measured by connecting one of the current electrodes to an ammeter to measure the amount of current going into the earth. Another electrode is connected to a voltmeter next to the current electrode and placed at some distance,  $r$ , away from the electrode to measure the voltage difference between the two locations (Figure 2.2). The distance of current electrode,  $r_i$  must be large compared to voltage electrode,  $r_v$  (at least by 10 times). When  $r_i$  is small,  $r_v$  is smaller and the voltage drop is small (Burger, 1992; Robinson and Coruh, 1988; Telford et al., 1990).

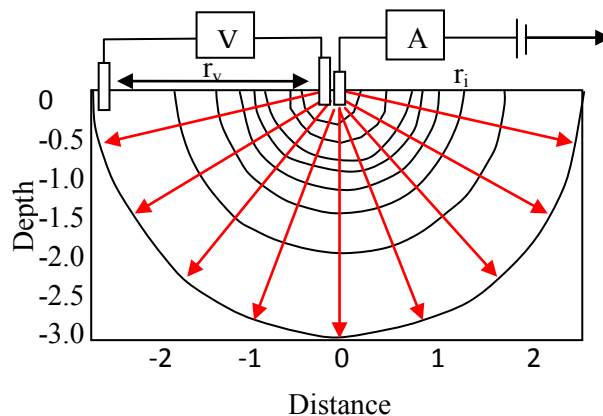


Figure 2.2: Measuring earth resistivity (modified after Burger, 1992; Robinson and Coruh, 1988; Telford et al., 1990).

### 2.1.1 Current flow from two closely spaced electrodes

By placing the two current electrodes close to each other, the current distribution and equipotentials produced within a homogeneous become more complicated. Instead of the current flowing radially out from the current electrode, it

flows along curved paths connecting the two current electrodes (Figure 2.3). Table 2.2 shows the proportion for the six paths labeled 1 through 6. From these calculations and the graph of the current flow shown, notice that almost 50% of the current placed into the ground flows through rock at depths shallower or equal to the current electrode spacing.

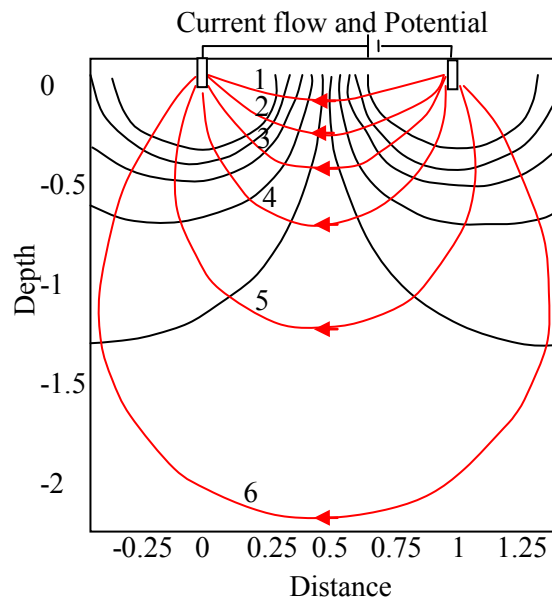


Figure 2.3: Equipotential surfaces (black lines) and current lines of flow (red lines) (modified after Burger, 1992; Robinson and Coruh, 1988; Telford et al., 1990).

Table 2.1: Current path and their percent of total current that penetrates into the depth of line (modified after Burger, 1992; Robinson and Coruh, 1988; Telford et al., 1990).

Current path	% of total current
1	17
2	32
3	43
4	49
5	51
6	57

### 2.1.2 Measuring earth resistivity

The resistivity in homogeneous earth can be estimated using two potential electrodes (purple) placed between the two current electrodes (red and green). Let the distances between the four electrodes be  $r_1$ ,  $r_2$ ,  $r_3$  and  $r_4$  as shown in Figure 2.4. The potential computed along the surface of the earth is shown in the Figure 2.5. The voltage observed with voltmeter is the difference in potential at the two voltage electrodes,  $\Delta V$  (Burger, 1990; Pozdnyakova and Zhang, 1999; Butler, 2001).

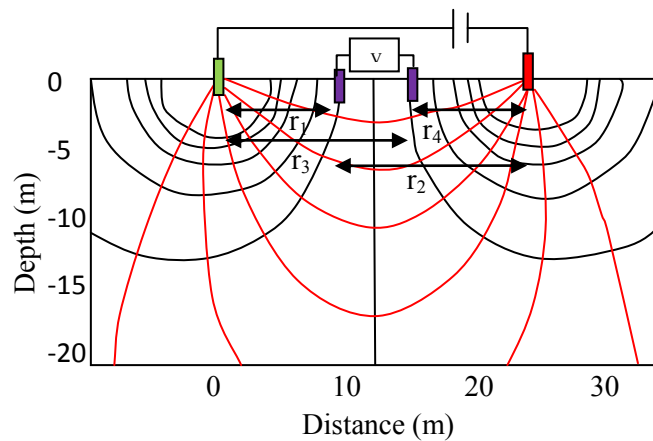


Figure 2.4: Four electrodes principle to measure resistivity or conductivity (modified after Burger, 1990; Pozdnyakova and Zhang, 1999; Butler, 2001).

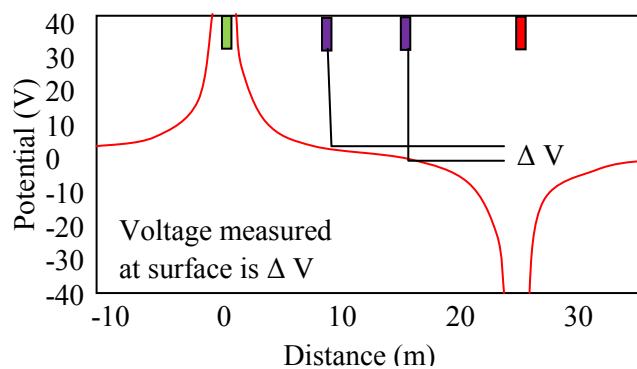


Figure 2.5: Potential along the surface and potential difference (modified after Burger, 1990; Pozdnyakova and Zhang, 1999; Butler, 2001).



Knowing the locations of four electrodes, and by measuring the amount of current input into the ground,  $i$ , and the voltage difference between the two potential electrodes,  $\Delta V$ , the apparent resistivity,  $\rho_a$ , of the medium can be calculated using equation (2.5) (Keller and Frischknecht, 1996).

$$\rho_a = \frac{2\pi\Delta V}{i} \left[ \frac{1}{\left(\frac{1}{r_1}\right) - \left(\frac{1}{r_2}\right) - \left(\frac{1}{r_3}\right) + \left(\frac{1}{r_4}\right)} \right] \quad (2.5)$$

### 2.1.3 Depth of penetration

When two current electrodes are moved close to one another, current flows along arc-shaped paths connecting the two electrodes. About 50% of the current flows through rock at depths shallower than the current electrode spacing provided the earth has a constant resistivity. By increasing the electrode spacing, more of the injected current will flow to greater depths. If the electrode spacing is much closer, current flows mostly near the earth surface and apparent resistivity will be dominated by resistivity structure of the near surface (Figure 2.6).

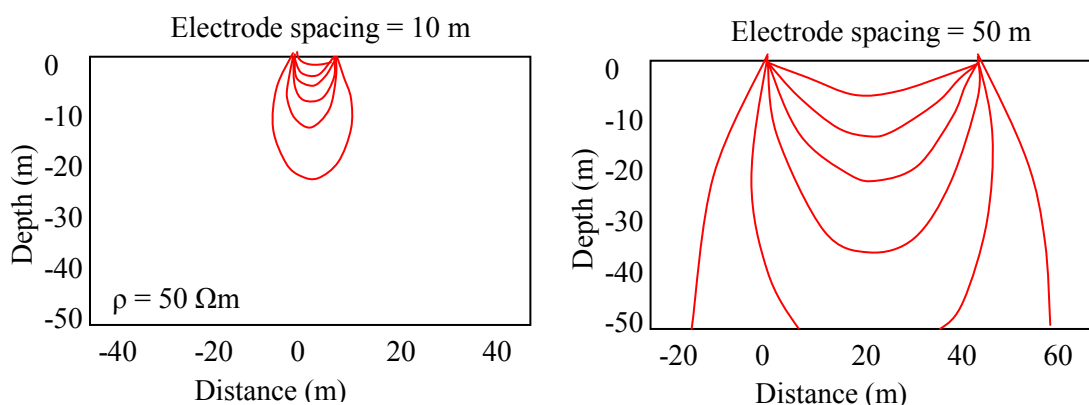


Figure 2.6: Current flow through the earth with different electrode spacing (modified after Burger, 1992).

### 2.1.4 Current flow in layered media

Assume that the resistivity change with depth can be quantized into a series of discrete layers, each with a constant resistivity. Figure 2.7 shows high resistivity layer ( $250 \Omega\text{m}$ ) overlying a lower resistivity layer ( $50 \Omega\text{m}$ ). This model is associated with unsaturated alluvium overlying water saturated alluvium. Figure 2.8 shows a low resistivity layer ( $50 \Omega\text{m}$ ) overlying a higher resistivity layer ( $250 \Omega\text{m}$ ), associated with an aquifer. Assuming a homogeneous medium, the current paths from the two current electrodes are labeled as blue lines while red lines represent current paths in a two layer model. The current in Figure 2.7 appears to be pulled downward into the low resistivity layer ( $50 \Omega\text{m}$ ) while the current path in Figure 2.8 appears to be bent upward, trying to remain within the lower resistivity layer at the top of the model. For the model in Figure 2.7, that path goes through the deep layer while for a model in Figure 2.8, that path goes through the shallow layer. The current is distorted in such a way in the low resistivity layer (Burger, 1992).

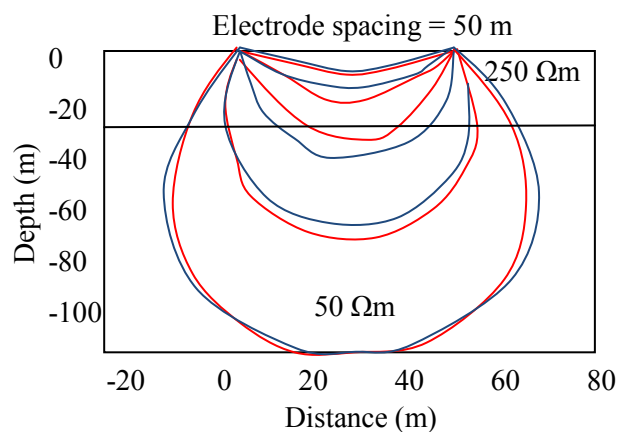


Figure 2.7: Current flows through a model of high resistivity overlying low resistivity layer (modified after Burger, 1992).

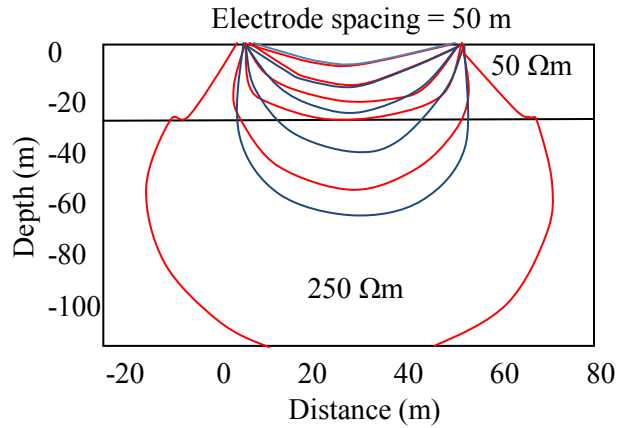


Figure 2.8: Current flows through a model of low resistivity overlying high resistivity layer (modified after Burger, 1992).

### 2.1.5 Current flow and current density

The distribution of current density exists when a horizontal interface is present. It is important to know the orientation of flow lines and equipotentials when crossing a boundary separating regions of different conductivity or resistivity. Hubbert, 1940 as cited by Burger, 1992 demonstrated that the flow lines follow a tangent relationship (2.6)

$$\frac{\tan \theta_1}{\tan \theta_2} = \frac{\rho_2}{\rho_1} \quad (2.6)$$

Where  $\theta$  : refraction angle

$\rho$  : resistivity

If  $\rho_2$  of the deeper material is greater, the current flow lines bend in toward the normal to the interface (Figure 2.9(b)) and, as a consequence, are more widely spaced. However, if the reverse is true, Figure 2.9(c) shows the current flow lines bent away from the normal, become oriented more parallel to the interface, and are closer together. Figure 2.10(a) illustrates the pattern of current flow lines for a

homogeneous subsurface ( $\rho_2 = \rho_1$ ). If  $\rho_2$  is increased, more current will flow above the interface, the current flow lines will be spaced more closely, and the current density will be greater in the region above the interface relative to the case of the homogeneous subsurface (Figure 2.10(b)). If  $\rho_2 < \rho_1$ , a greater percentage of current will flow beneath the interface, the current flow lines will be spaced more widely in the material above the interface, and the current density will be reduced (Figure 2.10(c)).

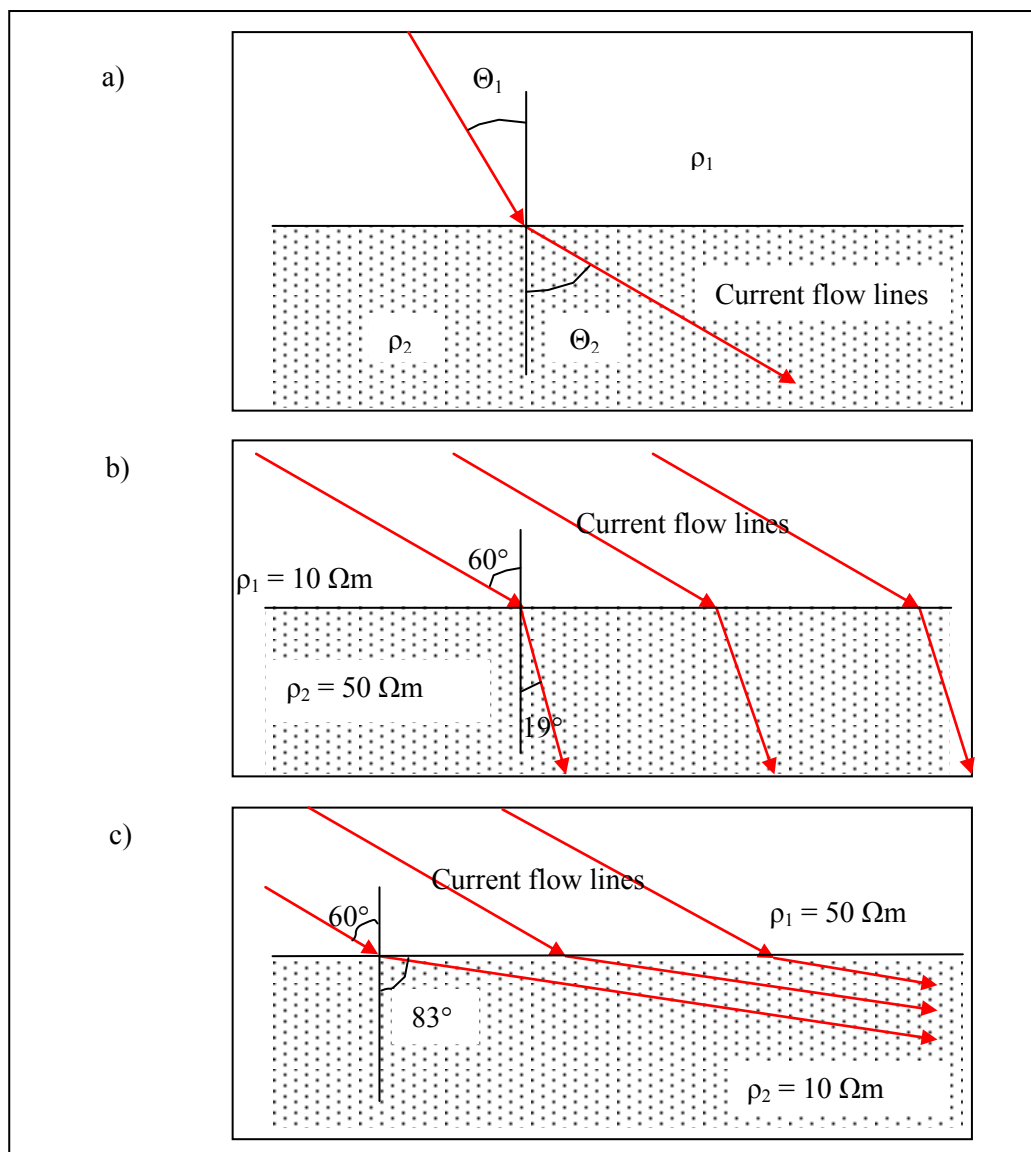


Figure 2.9: Refraction of current flow lines at a boundary separating materials of different resistivity. (a) Symbols used in equation 3.6, (b) Refraction when  $\rho_1 < \rho_2$ , (c) Refraction when  $\rho_1 > \rho_2$  (modified after Burger, 1992).

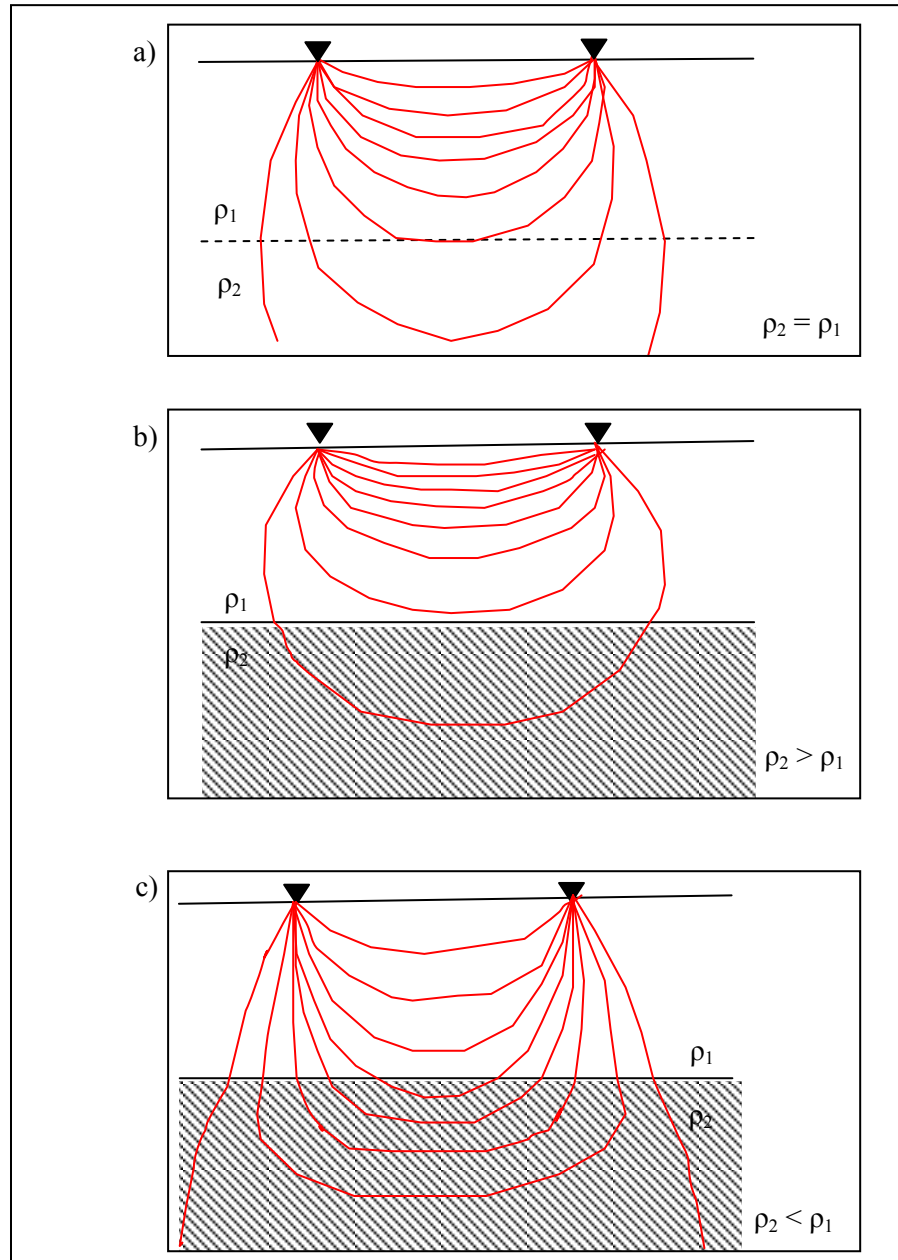


Figure 2.10: Qualitative distribution of current flow lines when a horizontal interface separates materials of different resistivities. (a) Homogeneous subsurface, (b)  $\rho_2 > \rho_1$ , (c)  $\rho_2 < \rho_1$  (modified after Burger, 1992).

### 2.1.6 Current flow and electrode spacing

A series of four experiments is conducted, each centered at the same point. Initially, current electrodes are kept closely spaced. Current and voltages are

measured and then the apparent resistivity is computed. Then the same experiment is repeated but the current electrode spacing is systematically increased. Consider the earth model a high resistivity layer over a lower resistivity layer (Figure 2.11).

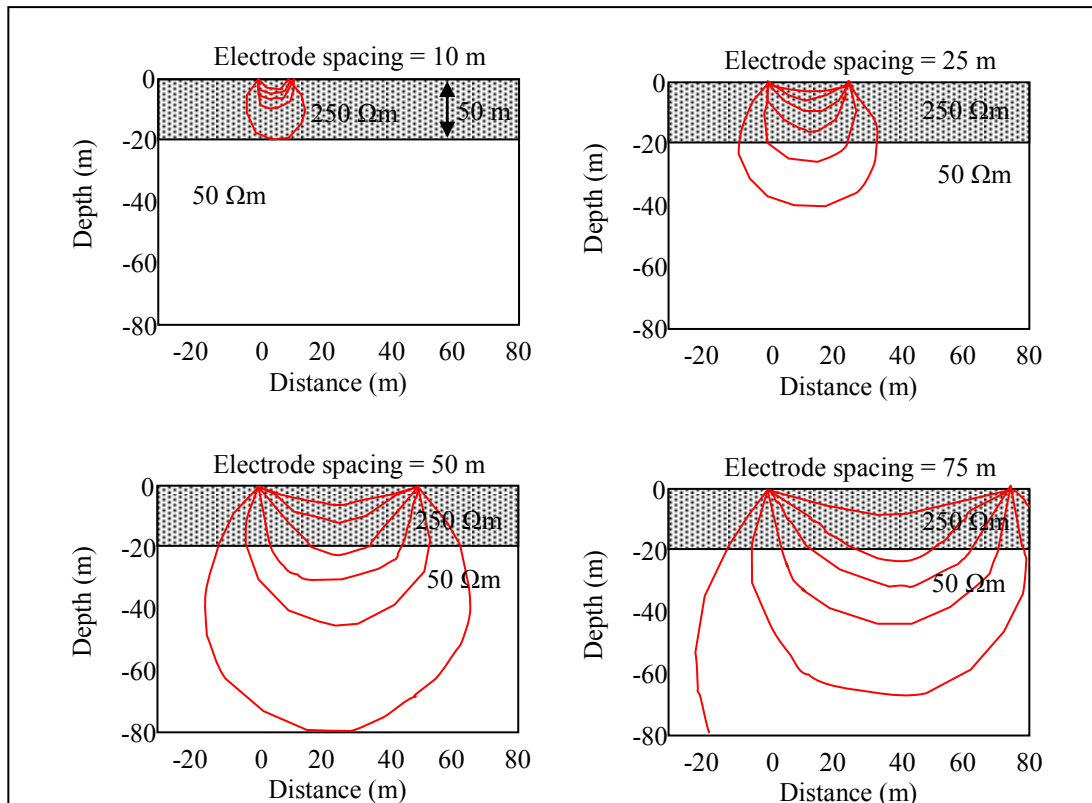


Figure 2.11: Current flow through different resistivity medium with different electrode spacing (modified from Burger, 1992).

When the current electrodes are closely spaced, most of the current flows through the upper layer along paths that are very close to those if the model were homogeneous. The current flow looks like that found in a homogeneous medium because there is not enough current flow to detect the deeper, lower resistivity layer. The computed apparent resistivity will be very close to the resistivity of the upper layer.

Now, the current electrode spacing is increased. At larger spacing, more current flows to greater depths. Thus, the presence of the lower resistivity layer

begins to affect a greater portion of the current. In this case, current is preferentially drawn downward into the lower resistivity layer, decreasing the current density between the two current electrodes where voltage measurement is taken. This decrease in current density is because our computed values of apparent resistivity decreases from 250  $\Omega\text{m}$  (Burger, 1992).

At very large current electrode spacing, all the current flows through the lower resistivity layer (lower medium). As observed for the very close electrode spacing, current flowing along the lines are similar to those found in a homogeneous medium. However, the medium has a resistivity of 50  $\Omega\text{m}$ , not 250  $\Omega\text{m}$ . Figure 2.12 shows as the current electrode spacing is increased, the apparent resistivity will decrease, eventually approaching 50  $\Omega\text{m}$ .

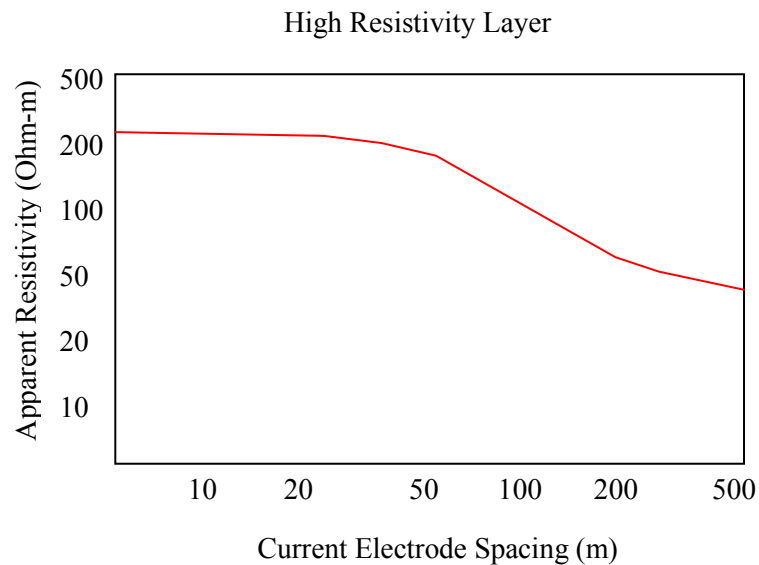


Figure 2.12: Apparent resistivity with electrode spacing in high resistivity layer (Mooney, 1958 as cited by Reynolds, 1997).

In another experiment, a low resistivity layer overlies a higher resistivity layer as shown in Figure 2.13 to see how apparent resistivity vary with varying electrode spacing. When current electrodes are very close, most of the current flows

through the upper layer until it essentially behaves like it would in a homogeneous earth. The computed apparent resistivity will be very close to the resistivity of the upper layer,  $50 \Omega\text{m}$  (Burger, 1992).

At larger current electrode spacing, more current flows to greater depth. Thus, the presence of higher resistivity layer begins to affect a greater portion of the current. This occurs even though current prefers to flow through the lower resistivity layer (upper layer). Despite these greater electrodes spacing, current would still flow through the upper layer, compared to the current density that would have been produced in a homogeneous half space. At these larger electrodes spacing there is a greater current density near the potential electrodes. This relative increase in current density will cause our computed value of apparent resistivity to increase to more than  $50 \Omega\text{m}$ .

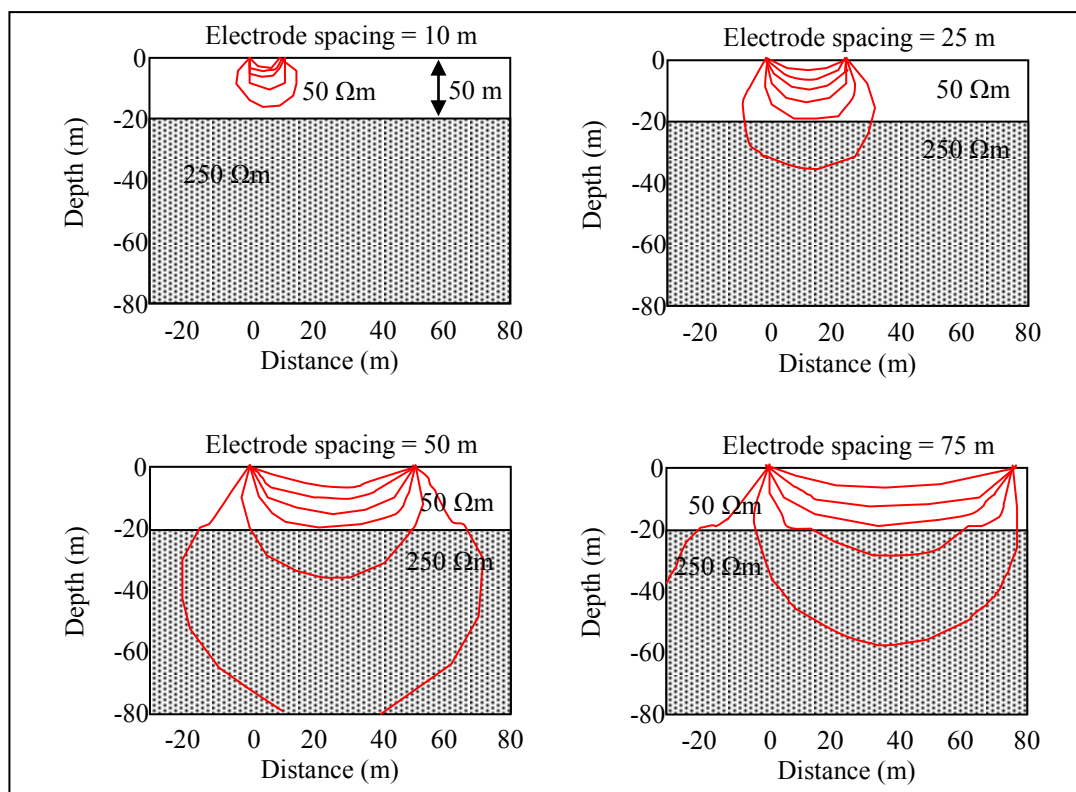


Figure 2.13: Current flow through lower to higher resistivity medium with different electrode spacing (modified after Burger, 1992).



At very large current electrode spacing, all the current flows through the higher resistivity layer in the lower medium. In this case, the current flows along lines that are similar to those found in a homogeneous medium. However, the medium has a resistivity of 250  $\Omega\text{m}$ . Thus, as the current electrode spacing is increased, the apparent resistivity will increase, eventually approaching 250  $\Omega\text{m}$  (Figure 2.14) because the current would prefer to flow within the first layer, notice that the apparent resistivity approaches the resistivity of the layer more slowly with greater electrode spacing (Mooney, 1958 as cited by Reynolds, 1997).

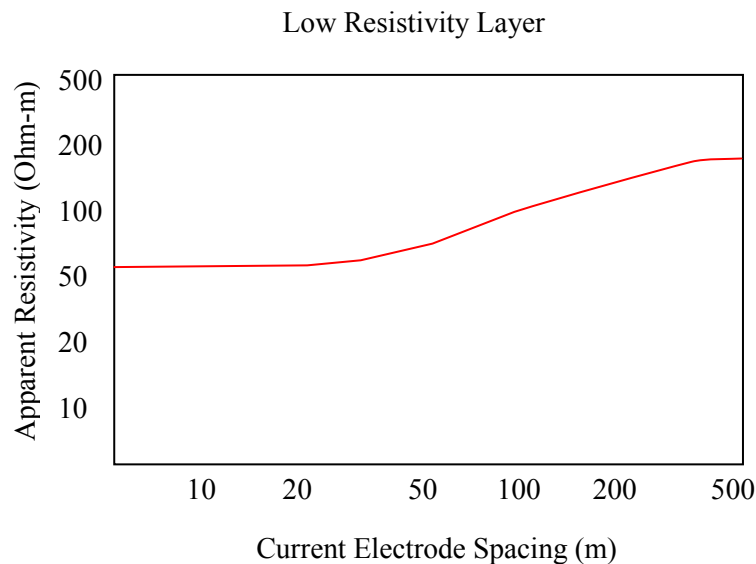


Figure 2.14: Apparent resistivity with electrode spacing in low resistivity layer (Mooney, 1958 as cited by Reynolds, 1997).

### 2.1.7 Resistivity arrays

The resistivity method has its origin in the 1920's due to the work of the Schlumberger brothers. Approximately for the next 60 years since then, for quantitative interpretation, conventional sounding surveys (Reynolds, 1997) were normally used. In this method, the centre point of the electrode array remains fixed,

but the spacing between the electrodes is increased to obtain deeper information about the subsurface. Figure 2.15 shows common arrays used in resistivity surveys and their geometric factors.

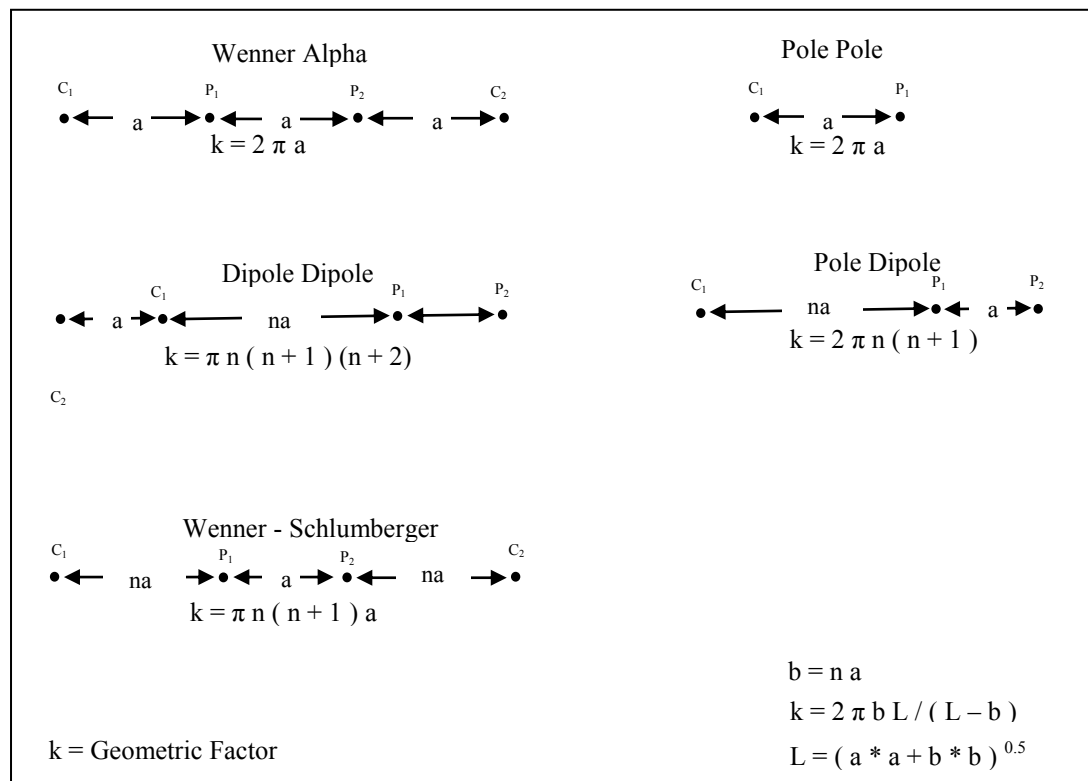


Figure 2.15: Common arrays used in resistivity surveys and their geometric factors.

The measured apparent resistivity values are normally plotted on a log-log graph paper. To interpret the data from a survey, it is normally assumed that the subsurface consists of horizontal layers. In this case, the subsurface resistivity changes only with depth, but does not change in the horizontal direction. A one-dimensional (1-D) model of the subsurface is used to interpret the measurement (Figure 2.16(a)). Figure 2.17 shows an example of the data from a sounding survey and a possible interpretation model. Despite this limitation, this method has given useful results for geological situations where the 1-D model is approximately true. Another classical survey technique is the profiling method. In this case, the spacing